Available online at www.sciencedirect.com
SCIENCE DIRECT
International Journal of Pharmaceutics 316 (2006) 162–169
INTERNATIONAL JOURNAL OF PHARMACEUTICS
www.elsevier.com/locate/ijpharm

Pharmaceutical Nanotechnology

Potential use of drug carried-liposomes for cancer therapy via direct intratumoral injection

Ande Bao [a,b,*], William T. Phillips [b], Beth Goins [b], Xiangpeng Zheng [c], Sarmad Sabour [a], Mohan Natarajan [a], F. Ross Woolley [b], Cristina Zavaleta [b], Randal A. Otto [a]

[a] *Department of Otolaryngology – Head and Neck Surgery, University of Texas Health Science Center at San Antonio, San Antonio, TX 78229-3900, USA*
[b] *Department of Radiology, University of Texas Health Science Center at San Antonio, San Antonio, TX 78229-3900, USA*
[c] *Department of Radiation Oncology, University of Texas Health Science Center at San Antonio, San Antonio, TX 78229-3900, USA*

Received 27 October 2005; received in revised form 17 February 2006; accepted 20 February 2006
Available online 31 March 2006

Abstract

Liposomes have recognized advantages as nano-particle drug carriers for tumor therapy. In this study, the pharmacokinetics and distribution of intratumorally administered liposomes were investigated as drug carriers for treating solid tumors via direct intratumoral administration. ^{99m}Tc-liposomes were administered intratumorally to nude rats bearing human head and neck squamous cell carcinoma xenografts. Planar gamma camera images were analyzed to evaluate the local retention of the intratumorally administered liposomes. Co-registered pinhole micro-single photon emission computed tomography (SPECT)/computed tomography (CT) images were acquired of the whole animal as well as the dissected tumors to determine intratumoral distribution of the ^{99m}Tc-liposomes. For ^{99m}Tc-liposomes, there was an initial retention of $47.4 \pm 11.0\%$ ($n = 4$) in tumors and surrounding tissues. At 20 h, $39.2 \pm 10.6\%$ ($n = 4$) of ^{99m}Tc-activity still remained in the tumor. In contrast, only $18.7 \pm 3.3\%$ ($n = 3$) of the intratumoral ^{99m}Tc-activity remained for unencapsulated ^{99m}Tc-complex at 20 h. Pinhole micro-SPECT images demonstrated that ^{99m}Tc-liposomes also have a superior intratumoral ^{99m}Tc-activity diffusion compared with unencapsulated ^{99m}Tc-complex. Higher intratumoral retention of ^{99m}Tc-liposomes accompanied by an improved intratumoral diffusion suggests that intratumorally administered liposomal drugs are potentially promising agents for solid tumor local therapy.

Keywords: Liposomes; Intratumoral administration; Drug delivery; Nuclear imaging; Micro-SPECT; Micro-CT

1. Introduction

Liposomes have been recognized as an effective nano-particle drug delivery system for nearly four decades (Gregoriadis, 1976a,b). Due to their unique characteristics, liposomes are employed to deliver a variety of agents because of their improved therapeutic characteristics when compared to their delivery by other methods. More recently, developments in liposome technology are leading to a burgeoning number of promising experimental and clinical applications (Torchilin, 2005). The liposomes approved to date for clinical use by the U.S. Food and Drug Administration (FDA) are used primarily to deliver cancer therapy drugs and antibiotics (Allen and Cullis, 2004). In addition to transporting anti-cancer drugs, anti-bacterials or anti-fungals, liposomes have been investigated as a non-viral vehicle for reaching targeted cells when performing gene therapy (Noguchi et al., 1998), and as antigen carriers for immunization (Therien et al., 1990).

The in vivo pharmacokinetics and organ distribution of drug-containing liposomes can be identified by labeling them with photon-emitting radionuclides, which makes it possible to carry out multiple assessments with non-invasive imaging techniques in the same animal across different points in time (Gabizon et al., 2003). Recently, a method was reported for radiolabeling liposomes possessing high efficiency and specific activity for both technetium-99m (^{99m}Tc) and rhenium-186 (^{186}Re) using their *N*,*N*-bis(2-mercaptoethyl)-*N*′,*N*′-diethyl-ethylenediamine (BMEDA) complexes (Bao et al., 2003a,b, 2004). One of the

Abbreviations: HNSCC, head and neck squamous cell carcinoma; SPECT, Single Photon Emission Computed Tomography; CT, Computed Tomography; BMEDA, *N*,*N*-bis(2-mercaptoethyl)-*N*′,*N*′-diethyl-ethylenediamine

* Corresponding author at: Department of Otolaryngology, University of Texas Health Science Center at San Antonio, 7703 Floyd Curl Drive, San Antonio, TX 78229-3900, USA. Tel.: +1 210 567 5657; fax: +1 210 567 3617.
E-mail address: bao@uthscsa.edu (A. Bao).

0378-5173/$ – see front matter © 2006 Elsevier B.V. All rights reserved.
doi:10.1016/j.ijpharm.2006.02.039

significant advantages of this labeling method is that it can be used to directly label the liposomes carrying encapsulating drugs without the need for pre-labeling processing. Thus, the pharmacokinetics of a variety of liposomal drugs, such as Doxil®, may be studied with ^{99m}Tc-labeling (Bao et al., 2004). ^{99m}Tc is the most commonly used radionuclide in clinical nuclear medicine. This radionuclide has a 6.0 h half-life emitting 141 keV gamma rays, an ideal energy for gamma camera imaging scanners.

A model for studying the in vivo characteristics of ^{99m}Tc-liposomes following intratumoral administration was developed using male *rnu*/*rnu* athymic nude rats (Harlan, Indianapolis, IN) at 4–5 weeks age (75–100 g). Each rat had previously been injected with human head and neck squamous cell carcinoma (HNSCC) cells subcutaneously on the dorsum at the level of the scapulae. The animals all bore established palpable tumors at the time of the study.

Using the labeling method noted above, the in vivo behavior of ^{99m}Tc-liposomes following direct intratumoral injection to the HNSCC xenografts in the rats was studied. The retention of ^{99m}Tc-liposomes in the tumor and surrounding areas at different times was calculated from parallel hole collimator-planar gamma camera images acquired using a combined micro-single photon emission computed tomography and computed tomography scanner (micro-SPECT/CT) for small animal imaging. High-resolution pinhole SPECT images of both in vivo and dissected tumors at 1.21 mm image resolution with subsequent co-registered CT images were acquired to study the intratumoral distribution of ^{99m}Tc-activity. The radioactivity present in the dissected tumors, adjacent tissues as well as in the animal's major internal organs at 24 h after administration was also measured using a gamma well counter.

2. Materials and methods

2.1. HNSCC xenografts in nude rats

The animal experiments reported in the present paper were performed according to the NIH Animal Use Guidelines and were approved by the University of Texas Health Science Center at San Antonio (UTHSCSA) Institutional Animal Care Committee. During all invasive and restrained animal-handling procedures, i.e. tumor cell inoculation, radiotracer injection and animal imaging, the animals were anesthetized with 1–3% of isoflurane (Vedco, St Joseph, MO) in 100% oxygen using an anesthesia inhalation machine (Bickford, Wales Center, NY). The head and neck squamous cell carcinoma cell line, SCC-4, used for HNSCC tumor model is an established human-origin tumor cell line provided by Martin Thornhill, PhD, of the UTHSCSA, School of Dentistry. It was originally obtained from American Type Culture Collection (ATCC, Manassas, VA). The HNSCC tumor model described in the current research had previously been characterized as a typical squamous cell carcinoma via hematoxylin–eosin (HE) staining and immunohistochemistry of epidermal growth factor receptor (EGFR).

SCC-4 Cells were cultured in Dulbecco's Modified Eagle's Medium (Invitrogen, San Diego, CA) containing 10% fetal bovine serum, 2 mM L-glutamine, and antibiotics (penicillin and streptomycin) in 100 mm × 20 mm Corning cell culture dishes (Corning Inc, Corning, NY) at 37 °C in a 5% CO_2 atmosphere. When near confluence, cells were trypsinized and collected to determine the number of cells and viability by Trypan Blue dye exclusion assay. The appropriate volume of cell suspension was transferred to a new tube and centrifuged at 800 rpm in an Allegra 21R Centrifuge (Beckman Coulter, Fullerton, CA) at 4 °C for 5 min. Following aspiration of the supernatant, the cell pellets were diluted with saline for injection (Abbott Laboratories, Abbott Park, IL) to a concentration of 5×10^6 cells in 0.2 ml saline. Aliquots of 0.2 ml cell suspension were drawn into tuberculin syringes in preparation for the tumor cell inoculation.

To grow the HNSCC xenografts, each male *rnu*/*rnu* athymic nude rat (Harlan, Indianapolis, IN) at 4–5 weeks age (75–100 g) was inoculated subcutaneously with 5×10^6 of SCC-4 tumor cells in 0.20 ml of saline on the dorsum at the level of the scapulae. The animals were fed and housed following the protocol for the nude rat living environment at the animal facility at UTHSCSA, and were checked daily after tumor cell inoculation. When the tumor growth in each animal was palpable and of sufficient size to be measured using calipers, the tumor size was obtained by measuring the length (l), width (w) and thickness (t) of each tumor. The tumor volumes were subsequently calculated using the ellipsoid volume formula, $V = (\pi/6)lwt$ (Tomayko and Reynolds, 1989). When the tumor volume reached approximately 1 cm^3, which typically occurred between 13 and 14 days after tumor cell inoculation, the tumor bearing animals were then used for study.

2.2. Preparation of the liposomes

Liposomes with a nominal diameter of 100 nm containing 300 mM of ammonium sulfate (Sigma, St Louis, MO) and 10 mg/ml of patent blue dye (Sigma, St Louis, MO) comprised of distearoylphosphatidylcholine (DSPC) (Avanti Polar Lipids, Pelham, AL) and cholesterol (Calbiochem, San Diego, CA) having a molar ratio of 56:44 were prepared and characterized using the process previously described by Bao et al. (2003b). Following manufacture, the liposome particle diameter was 122.1 ± 5.5 nm prior to radiolabeling as measured using a 488 nm laser light scattering instrument (Brookhaven Instruments, Holtsville, NY).

2.3. Preparation of ^{99m}Tc-N,N-bis(2-mercaptoethyl)-N′,N′-diethyl-ethylenediamine (BMEDA)

The method used to prepare the ^{99m}Tc-BMEDA was the same as previously described by Bao et al. with minor modifications (2004). In brief, the process proceeded as follows: 50 mg of sodium glucoheptonate (GH) (Sigma, St Louis, MO) and 3.5 μl of BMEDA (synthesized in house) were combined in the same vial, followed by the addition of 5.0 ml of normal saline for injection (nitrogen gas-flushed in advance). Following 20 min of magnetic stir mixing, 65 μl of freshly prepared degassed stannous chloride (Aldrich, Milwaukee, WI) solution (12 mg/ml)

was added to the GH–BMEDA solution, followed by pH adjustment using 0.05 M of sodium hydroxide to achieve a pH ranging between 7 and 8. At that point, 1.0 ml of the resulting solution was transferred to a glass vial containing 0.60 ml of 2.22 GBq (60 mCi) ^{99m}Tc-pertechnetate (GE Healthcare, San Antonio, TX). The mixed solution was incubated at 25 °C for 20 min with intermittent gentle shaking. The labeling efficiency of the ^{99m}Tc-BMEDA was found to be over 80% employing paper chromatography eluted with methanol or saline. The ^{99m}Tc-BMEDA described above was used either by itself for animal study or for later liposome labeling employed in animal study.

2.4. Preparation of ^{99m}Tc-liposomes

For a typical labeling study, 1.0 ml of liposomes (60 mM of total lipids) prepared as described above were separated to remove free ammonium sulfate from liposomes by elution with phosphate buffered saline (PBS), pH 7.4 via disposable Sephadex G-25 column chromatography (Amersham Biosciences, Uppsala, Sweden). The product was added to the ^{99m}Tc-BMEDA solution and incubated at 37 °C for 1 h. Again, the ^{99m}Tc-liposomes were separated from any unencapsulated ^{99m}Tc-BMEDA via disposable Sephadex G-25 column chromatography eluted with PBS buffer, pH 7.4. The labeling efficiency of ^{99m}Tc-liposomes was 78.9%. The liposome particle diameter after labeling was 136.4 ± 13.1 nm.

2.5. Intratumoral distribution of ^{99m}Tc-liposomes and ^{99m}Tc-BMEDA after intratumoral administration

Nude rats bearing a tumor with an average volume of $0.94 \pm 0.21\,cm^3$ were injected intratumorally with 0.19 ± 0.04 ml of ^{99m}Tc-liposomes, which contained 1.7 ± 0.4 mg of DSPC and cholesterol, having 56.2 ± 11.8 MBq (1.52 ± 0.32 mCi) ^{99m}Tc-activity, using U-100 insulin syringes with $28G \times 1/2''$ needles (Becton Dickinson, Franklin Lakes, NJ). The ^{99m}Tc-liposome dose for each animal was divided and delivered to two separate locations in the tumor for better tumor coverage.

Planar gamma camera images, SPECT images and CT images were acquired using a micro-SPECT/CT scanner (XSPECT, Gamma Medica, Northridge, CA). Three minutes after the intratumoral administration, thirty 1-min frames of dynamic lateral view planar images were acquired using a parallel hole collimator. Subsequently, static images were collected at 2, 6 and 20 h after liposome administration with the same detector and animal positions as those used for dynamic image acquisition. Acquisition durations per image were: 2 min at 2 h; 4 min at 6 h; and 10 min at 20 h. During each planar image acquisition, a standard ^{99m}Tc-source was positioned outside the animal but still within the field of view for image quantification.

At 20 h following the intratumoral injection, immediately following planar image acquisition, 1-mm pinhole collimator SPECT images were acquired, with the center of the field of view (FOV) focused on the tumor of each animal. The radius of rotation (ROR) was 4.95 cm with a FOV of 6.78 cm. This was accomplished using 64 projections at 20 s per projection. The SPECT imaging was followed by CT image acquisition (X-ray source: 50 KVp, 600 mA; 256 projections) while precisely maintaining the positioning of the animal. The software provided with micro-SPECT/CT was used for the SPECT and CT image reconstruction including the SPECT/CT image fusion. The SPECT images were reconstructed to produce image sizes of $56 \times 56 \times 56$ with an image resolution of 1.21 mm. The CT images were also reconstructed, resulting in image sizes of $512 \times 512 \times 512$ with a 0.15 mm image resolution. The percentage of ^{99m}Tc activity retained in the tumor and the surrounding tissues across time was calculated from planar images created by drawing the region of interest (ROI) using the standard source as a point of reference.

Twenty-four hours following their intratumoral injection, each animal was euthanized by cervical dislocation. The major organs included the liver, spleen, kidneys, heart and lungs. The tumor itself, the skin immediately superior to the tumor and the muscle mass immediately inferior to the tumor were also collected. Activity at each of these sites was measured with a Wallac 1480 Wizard 3″ automatic well gamma counter (Perkin-Elmer Life Sciences, Boston, MA). The urine and feces excreted during the 24 h between tumor injection and euthanasia were also collected and the radioactivity of the total cumulated mass of excreta was measured. The percent of injected activity per gram of tissue or per organ was calculated as described by Bao et al. (2003b).

In order to study the effects of liposome encapsulation versus injection of unencapsulated ^{99m}Tc-BMEDA, a duplicate procedure was carried out using three nude rats also bearing a HNSCC tumor with a volume at $0.98 \pm 0.24\,cm^3$. As with the ^{99m}Tc-liposomes, the free ^{99m}Tc-BMEDA was administered intratumorally with 0.17 ± 0.09 ml of ^{99m}Tc-BMEDA containing 94.7 ± 50.3 MBq (2.56 ± 1.36 mCi) ^{99m}Tc-activity. To ensure that the study methods were comparable, all procedures, both ante and post-mortem, were duplicates of those carried out with animals receiving the encapsulated counterparts, ^{99m}Tc-liposomes. These included intratumoral administration, gamma camera imaging, CT image acquisition and organ distribution studies with identical time lines maintained for each activity from injection to post-mortem study.

2.6. Statistical analysis

The data are presented as the mean value ± one standard deviation (S.D.). Origin statistical software (Version 7.5) (Origin Lab, Northampton, MA) was used for the calculation of the means, standard deviations, and second order exponential decay curve simulation.

3. Results

3.1. Local retention behavior

Fig. 1 shows the planar gamma camera images of nude rats at five different times ranging from 3 min to 20 h following intratumoral administration of either ^{99m}Tc-liposomes or ^{99m}Tc-BMEDA. Both agents demonstrated much higher retention in

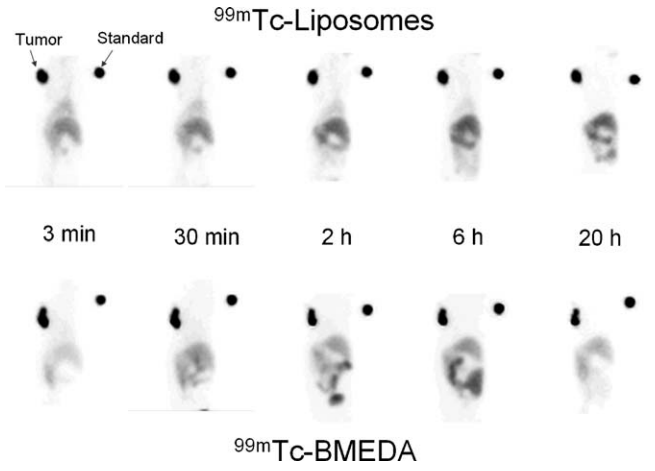

Fig. 1. Planar gamma camera images of tumor-bearing rats in a lateral position acquired at various times after intratumoral administration of ^{99m}Tc-liposomes or ^{99m}Tc-BMEDA. Tumors had much higher activity retention compared with all of the normal organs. ^{99m}Tc-BMEDA displayed a more rapid clearance through urine and feces compared with ^{99m}Tc-liposomes. Quantitative analysis demonstrates a much higher local retention ratio for ^{99m}Tc-liposomes.

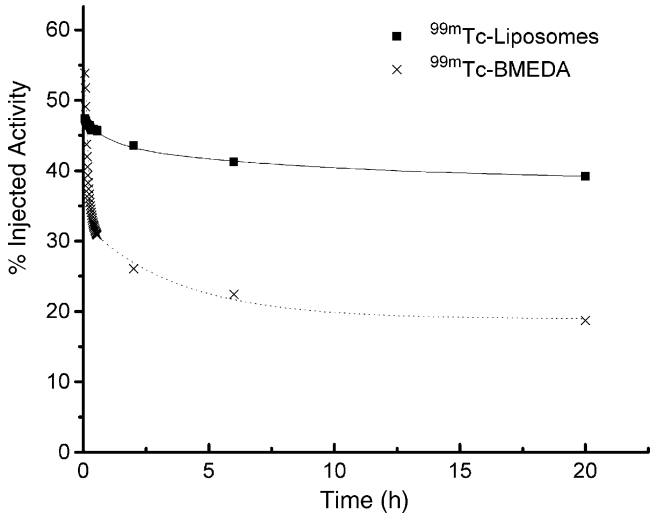

Fig. 2. Percent injected ^{99m}Tc-activity retained at local area at different times after intratumoral administration for ^{99m}Tc-liposomes (■) or ^{99m}Tc-BMEDA (X). The data was determined by ROI analysis of the planar images as shown in Fig. 1. The data points shown are the average values of four rats for ^{99m}Tc-liposomes and the average values of three animals for ^{99m}Tc-BMEDA (average ± S.D.). The curves are the simulated second order dual exponential decay curves for ^{99m}Tc-liposomes and ^{99m}Tc-BMEDA, respectively.

the tumors and the immediate surrounding area as compared with all other tissue sites at all times including the final antemortem measurements at 20 h after the initial administration. Approximately 53% of injected ^{99m}Tc-liposome activity cleared the local area immediately (Table 1) and then accumulated primarily in the liver and spleen. This distribution fate following tumor clearance is typical behavior for liposomes having the present formulation and lipid amount (Bao et al., 2003a,b). By contrast the ^{99m}Tc-BMEDA had a slower immediate clearance (∼28%) but a faster constant clearance (Table 1) with a large amount being excreted in urine and feces between 30 min and 6 h after administration. A quantitative analysis of the planar images demonstrated that ^{99m}Tc-liposomes had a very stable local retention from 3 min to 20 h after the initial immediate clearance of the liposomes. Although the unencapsulated ^{99m}Tc-BMEDA had a lower immediate clearance from the tumor area, its overall clearance half-life values were much shorter and intratumoral retention ratio was markedly lower as shown in Table 1.

^{99m}Tc-liposomes cleared from the injection site in two stages with 52.6 ± 12.2% (n = 4) of the injected activity cleared the administration site within 3 min. Of the remaining 47.4 ± 11.0% radioactivity in the tumor and surrounding tissues, a highly stable retention and slow clearance was displayed with 39.2 ± 10.6% (n = 4) of the ^{99m}Tc injected activity still remaining in the local area 20 h after administration (Fig. 2). Curve simulations on the intratumoral retentions of ^{99m}Tc-liposomes and ^{99m}Tc-BMEDA following the times after administration have shown that they both fitted very well with a second order exponential decay model (R^2 = 0.996 and 0.998, respectively). The data as presented in Fig. 2 are derived from a second order exponential decay model obtained by applying the following general formula:

$$y = y_0 + A_1\,e^{-x/t_1} + A_2\,e^{-x/t_2}$$

where: y_0 represents the Y offset (i.e. the constant retention activity other than the cleared components following the exponential decay mechanism), A_1 and A_2 represent the percentages of radioactivity which were cleared with the decay constants of t_1 and t_2 respectively for ^{99m}Tc-liposomes or ^{99m}Tc-BMEDA as calculated. Subsequently, the half clearance times correlated with the radioactivity components of A_1 and A_2 are t_1/0.693 and t_2/0.693 correspondingly.

The results shown in Table 1 suggest that following the immediate clearance of 51.5% of the liposomes, the remaining 48.5% of liposomes cleared from the injection site in the following phases: 2.1% of the injected activity cleared quickly from the injection site with a 0.07 h half clearance time; 7.3% cleared the injection site with a 3.2 h half time; and the residual 39.2% of injected activity is viewed as a permanent retention. Except for the initial rapid clearance as noted above, ^{99m}Tc-BMEDA had a much faster injection site clearance compared with ^{99m}Tc-liposomes (Fig. 2). There was only 18.7 ± 3.3% (n = 3) of injected ^{99m}Tc-BMEDA activity remaining at the

Table 1
Clearance characteristics of percent injected activities from tumors and the surrounding tissues after intratumoral administration of ^{99m}Tc-liposomes and ^{99m}Tc-BMEDA

Agent	Immediate clearance (%)	Phase I clearance ($T_{1/2}$)	Phase II clearance ($T_{1/2}$)	Constant retention (%)	R^2
^{99m}Tc-Liposomes	51.5	2.1% (0.07 h)	7.3% (3.2 h)	39.2	0.996
^{99m}Tc-BMEDA	27.6	39.8% (0.08 h)	13.7% (2.6 h)	18.9	0.998

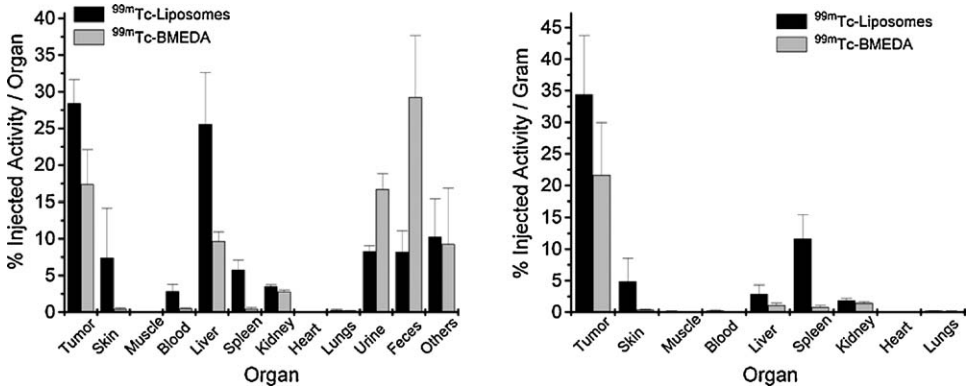

Fig. 3. Percent injected activity/organ (left) or percent injected activity/gram of tissue (right) of ^{99m}Tc-liposomes ($n=4$) and ^{99m}Tc-BMEDA ($n=3$) at 24 h after intratumoral administration. The radioactivities in skin and muscle were those in the tissues above or beneath the tumors.

injection site 20 h after administration. The second order exponential decay simulation supports the conclusion that 27.6% of injected activity cleared from the injection site immediately after administration; 39.8% cleared from local area with a 0.08 h half clearance time; and 13.7% of the injected ^{99m}Tc-BMEDA cleared from local area with a 2.6 h half clearance time, thus only 18.9% of injected ^{99m}Tc-BMEDA remained as a permanent retention fraction.

3.2. Organ distribution at 24 h

The distribution of the retention activity in the tumors and surrounding areas was evaluated at 24 h immediately after the animal was euthanized. These studies indicated that the greatest amount of the original injected ^{99m}Tc-liposome activity remained within the tumor itself (Fig. 3). The activity distribution was as follows: 28.4 ± 3.2% in the tumor mass; 7.4 ± 6.8%

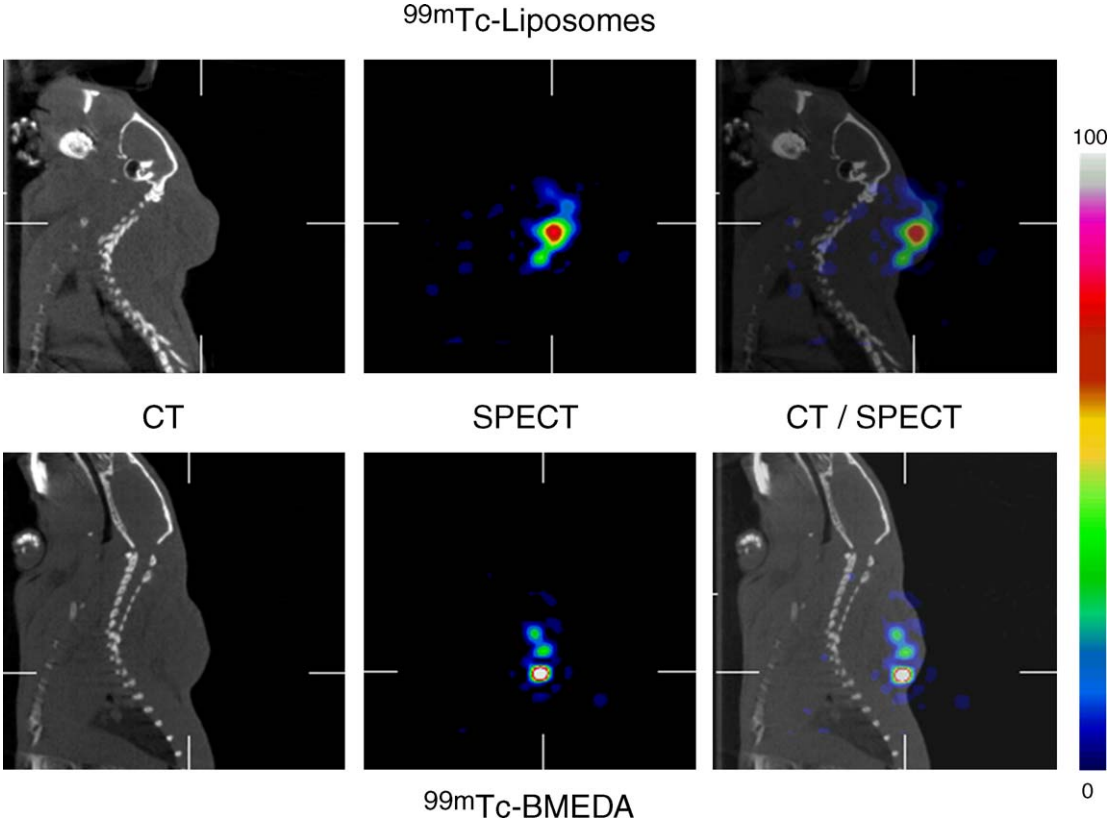

Fig. 4. Micro-CT, pinhole collimator SPECT and fused images of tumor-bearing rats acquired at 20 h after intratumoral administration of ^{99m}Tc-liposomes (upper panel) and ^{99m}Tc-BMEDA (lower panel). The pinhole collimator SPECT images were focused at the tumor in each animal. The color map shows the SPECT pixel values from 0 to the maximum expressed with an arbitrary value 100. The SPECT pixel values beyond the color range of the map are shown in white.

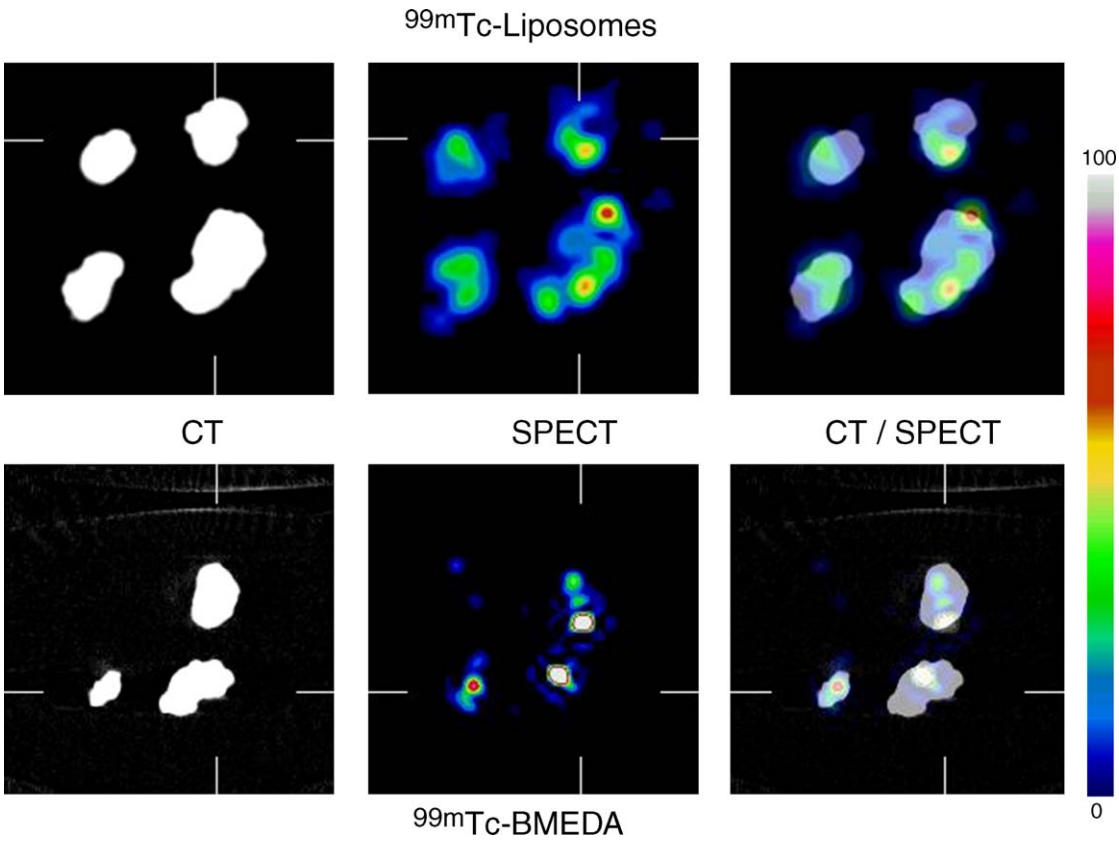

Fig. 5. Micro-CT, pinhole collimator SPECT and fused images of excised tumors after intratumoral administration of ^{99m}Tc-liposomes (upper panel) ($n=4$) and ^{99m}Tc-BMEDA (lower panel) ($n=3$). The images depict the intratumoral distribution of ^{99m}Tc-activity in the tumors from all of the animals at 24 h after administration after dissecting each tumor from each animal. The color map shows the SPECT pixel values from 0 to the maximum expressed with an arbitrary value 100. The SPECT pixel values beyond the color range of the map are shown in white.

in the extratumoral space between the mass and the skin; and $0.091 \pm 0.045\%$ in the muscle under the tumor ($n=4$ for all) for ^{99m}Tc-liposomes.

As with the ^{99m}Tc-liposomes, retention of injected ^{99m}Tc-BMEDA in the tumor and adjacent sites was studied 24 h after injection, immediately after the animal was euthanized. An evaluation of Fig. 3 identifying the percentage of activity per organ reveals that in the immediate area of the tumor the only meaningful activity for ^{99m}Tc-BMEDA was within the tumor itself. This totaled $17.4 \pm 4.7\%$ ($n=3$), which is a significantly lower intratumoral retention than ^{99m}Tc-liposomes ($P<0.05$). However the portion of Fig. 3 showing the percent of injected activity per gram for each organ clearly indicates higher intratumoral activities per gram of tissue for both ^{99m}Tc-liposomes and ^{99m}Tc-BMEDA compared with all other organs. These differences were statistically significant ($P<0.05$) for each site when compared to the tumor.

3.3. Intratumoral distribution at 20 h

Fig. 4 shows the micro-CT, micro-SPECT and their fused images of representative tumor-bearing rats at 20 h after administration of ^{99m}Tc-liposomes (upper panel) or ^{99m}Tc-BMEDA (lower panel). The pinhole collimator SPECT images were obtained by focusing on the tumors to obtain the intratumoral distribution and a high resolution of 1.21 mm was obtained. Fig. 5 shows the intratumoral activity distributions of the ^{99m}Tc-liposomes and ^{99m}Tc-BMEDA in the dissected tumors of all the animals included in the study at 24 h after injection. Interestingly, the relatively smaller molecules of the unencapsulated radiotracer, ^{99m}Tc-BMEDA was inferior in both uniformity and dispersion within the tumors compared with the 130 nm ^{99m}Tc-liposome nano-particles (Figs. 4 and 5). The intratumoral distribution pattern of ^{99m}Tc-liposomes is characterized by having not only the anticipated hot spots at the injection sites in the tumors, but also an unexpectedly broad interstitial diffusion within the tumors given that there were only two injection sites within each tumor. Assuming that this is a reliable characteristic of injected liposomes, their value as a drug delivery system for anti-tumor agents is significantly enhanced. By contrast, ^{99m}Tc-BMEDA activity was observed to remain confined to a comparatively limited area with noticeably less diffusion within the tumor. Based on these findings, it would appear that ^{99m}Tc-liposomes and ^{99m}Tc-BMEDA have different and potentially important intratumoral distribution and clearance characteristics due to factors that are currently not well understood.

4. Discussion

Direct drug administration using a variety of mechanisms ranging from surgical implantation to image-guided intralesional injection has received increasing interest in recent years.

Direct intratumoral delivery methods have significant potential advantages. Two of the most commonly cited are: (1) significantly higher local drug retention compared with systemic routes; (2) circumvention of the various physiological barriers to tumor drug delivery including the high interstitial pressure common to most solid tumors, which is also compounded by simultaneous drug excretion during drug transportation process (Nishikawa and Hashida, 1999; Jain and Baxter, 1988). The feasibility of directly injecting tumors has been greatly enhanced recently by the advances in imaging technology, which permit the use of image guided intervention systems. These image guided systems makes it possible to introduce therapeutic agents into areas once believed to be inaccessible without unacceptable risks.

As an important nano-particle carrier system, liposomes have been previously studied as delivery agents for intratumoral administration for non-viral gene delivery. A liposomal anticancer gene, E1A, was intratumorally administered for human HNSCC gene therapy and a moderate tumor response was observed (Villaret et al., 2002). Using pegylated liposomes containing surface diethylene-triamine-pentaacetate (DTPA) conjugation, the in vivo distribution of ^{99m}Tc-labeled liposomes in head and neck cancer xenograft bearing nude mice was studied after intratumoral administration (Harrington et al., 2000). At 24 h after administration, $34.7 \pm 8.8\%$ of injected activity remained in the tumor and there was much higher injected activity per gram of tissue in tumor compared with normal tissues. A previous pharmacokinetic study with an ovarian cancer xenograft had shown that by using liposomes composed of egg phosphatidylcholine (egg PC) and 1,2-dioleoyl-*sn*-glycero-3-phosphatidylethanolamine (DOPE) (1:1, mol/mol) with a particle diameter of 120.0 ± 15.2 nm, 35–50% of injected liposomes quickly left the injection site and were observed in the venous system within 1 min after administration. However, 10–40% of the injected liposomes remained in the tumors at 2 h (Nomura et al., 1998). This study also showed much higher intratumoral retention for cationic liposomes and liposomes with larger particle sizes. In these previous studies, there has been no report of the detailed intratumoral distribution of liposomes after intratumoral injection.

In the present study using a HNSCC xenograft, liposomes composed of DSPC and cholesterol with particle sizes of 136.4 ± 13.1 nm demonstrated a similar behavior with about 50% of the injected activity leaving the immediate injection area within 3 min followed by a slow subsequent clearance. Ultimately about 40% of injected activity remained in the tumor area at 20 h. There was a much lower ratio of injected drug dose per gram of tissue in each major non-cancerous organ, such as the liver and kidneys, compared with the tumor (Fig. 3); thus a much higher tumor drug dose compared with normal tissues, and a lower normal tissue toxicity are expected if a liposomal drug is used.

One of the practical challenges in using an intratumoral injection to perform tumor therapy is to ensure that the injected drugs distribute throughout the whole tumor assuring that all of the cancerous cells are killed. Use of high resolution imaging techniques, such as SPECT and positron emission tomography (PET), can provide the detailed intratumoral distribution information using a radiolabeled agent. In addition, noninvasive imaging techniques may also be important tools for the planning of the proposed intratumoral injection procedures, such as how many injection points are required and where the injection sites are located for optimum coverage for tumor therapy. High-resolution SPECT studies on the HNSCC tumors showed that ^{99m}Tc-liposomes had a broad intratumoral diffusion, which would clearly be beneficial in providing uniformly dispersed liposomal drugs throughout the tumor (Jain and Baxter, 1988).

As stated previously in Section 3, we observed a better intratumoral distribution with ^{99m}Tc-labeled liposomes compared with a small molecule, ^{99m}Tc-BMEDA. Liposomes appear to diffuse through an extended area of the solid tumor. This differs in comparison with ^{99m}Tc-BMEDA, which remains localized in a small area. Although the specific reasons for the observed differences between ^{99m}Tc-labeled liposomes and ^{99m}Tc-BMEDA are yet to be answered, the following speculations may explain this behavior: (1) the relatively larger size of liposomes and their lower interaction with surrounding extracellular matrix during convection-mediated liposome infusion give liposomes the capability of perfusing throughout the tumor interstitial space; thus a better intratumoral distribution; (2) the large particle size of liposomes compared with a small molecule, results in liposomes having a much slower clearance from interstitial space, which could lead to the higher intratumoral retention; (3) small molecules have a faster clearance dynamics from well-perfused regions of the tumor compared to liposomes; thus at 20 h after administration, only small areas within the tumor that have a very low diffusion efficiency remain.

It is apparent that future studies will need to address methods of improving the retention of liposomes within the tumor. However, the behavior of ^{99m}Tc-liposomes immediately following intratumoral injection suggests that this drug administration method is not limited to direct intratumoral therapy of large tumors. The rapid clearance of approximately 50% of the injected active agent indicates that a significant portion of the dose becomes a systemic agent. Consequently, it is entirely reasonable to consider the possibility of treating small tumors and distant metastases systemically as the active agent enters the blood and lymphatic circulation (Ueno et al., 2002).

Based upon current and prior observations among the authors and the physiological properties of the tissues involved, the reason for the relatively high activity between the tumor and the skin above the tumor may be explained by two factors. First is that HNSCC is a subcutaneous xenograft and in the animal model used in this research, a patent physiologic contact exists between the tumor and the skin above it. Secondly the location of the xenograft between the tumor and the skin is an area with relatively poor circulation. It is likely that in the case of a spontaneous tumor with an autologous blood supply, the local administration method may have a distinct advantage in drug delivery. The infusion of the injected drug carried liposomes into a central region of the tumor with poor vascularity will deliver a significantly higher dose than that achieved by the traditional intravenous administration route, thus providing another poten-

tial means for enhancing therapy in areas that are often difficult to access.

Tc and Re are in the same elemental group in the periodic table and share a similar chemistry. ^{99m}Tc is the most widely clinically used diagnostic radionuclide. Re has two promising radionuclides, ^{186}Re and ^{188}Re, which have excellent characteristics for tumor radionuclide therapy (Zweit, 1996). The beta particles emitted by therapeutic radionuclides, ^{186}Re and ^{188}Re, penetrate 1.80 and 4.20 mm (90% beta energy deposition) respectively in solid tumors (Prestwich et al., 1989). ^{99m}Tc-BMEDA and ^{186}Re-BMEDA are both ^{99m}Tc/^{186}Re-"SNS/S" type complexes. Previous studies on ^{99m}Tc-"SNS/S" and ^{186}Re-"SNS/S" complexes have demonstrated the same coordinate structure and a similar in vivo behavior (Pirmettis et al., 1996; Pelecanou et al., 1999). Our previous studies have shown that both ^{99m}Tc-BMEDA and ^{186}Re-BMEDA could be used for labeling liposomes with high labeling efficiency and high specific activity (Bao et al., 2003a,b, 2004). Given the similar in vitro and in vivo behavior of ^{99m}Tc-liposomes and ^{186}Re-liposomes labeled with ^{99m}Tc-BMEDA or ^{186}Re-BMEDA, ^{99m}Tc-liposomes should continue to be used as a model to investigate more fully the potential of ^{186}Re/^{188}Re-liposomes for tumor radionuclide therapy.

In summary, radiolabeled liposomes administered intratumorally were found to have a high intratumoral retention compared with normal organs. These intratumoral distribution studies have shown that radiolabeled liposomes also have promising interstitial diffusion after intratumoral administration. The present research also demonstrates the potential of using drug carried liposomes to perform systemic tumor radionuclide therapy via intratumoral administration route.

References

Allen, T.M., Cullis, P.R., 2004. Drug delivery systems: entering the mainstream. Science 303, 1818–1822.

Bao, A., Goins, B., Klipper, R., Negrete, G., Mahindaratne, M., Phillips, W.T., 2003a. A novel liposome radiolabeling method using ^{99m}Tc-"SNS/S" complexes: in vitro and in vivo evaluation. J. Pharm. Sci. 92, 1893–1904.

Bao, A., Goins, B., Klipper, R., Negrete, G., Phillips, W.T., 2003b. ^{186}Re-liposome labeling using ^{186}Re-SNS/S complexes: in vitro stability, imaging, and biodistribution in rats. J. Nucl. Med. 44, 1992–1999.

Bao, A., Goins, B., Klipper, R., Negrete, G., Phillips, W.T., 2004. Direct ^{99m}Tc labeling of pegylated liposomal doxorubicin (Doxil) for pharmacokinetic and non-invasive imaging studies. J. Pharmacol. Exper. Ther. 308, 419–425.

Gabizon, A., Shmeeda, H., Barenholz, Y., 2003. Pharmacokinetics of pegylated liposomal doxorubicin: review of animal and human studies. Clin. Pharmacokinet. 42, 419–436.

Gregoriadis, G., 1976a. The carrier potential of liposomes in biology and medicine (part one of two parts). N. Engl. J. Med. 295, 704–710.

Gregoriadis, G., 1976b. The carrier potential of liposomes in biology and medicine (part two of two parts). N. Engl. J. Med. 295, 765–770.

Harrington, K.J., Rowlinson-Busza, G., Syrigos, K.N., Uster, P.S., Vile, R.G., Stewart, J.S.W., 2000. Pegylated liposomes have potential as vehicles for intratumoral and subcutaneous drug delivery. Clin. Cancer Res. 6, 2528–2537.

Jain, R.K., Baxter, L.T., 1988. Mechanisms of heterogeneous distribution of monoclonal antibodies and other macromolecules in tumors: significance of elevated interstitial pressure. Cancer Res. 48, 7022–7032.

Nishikawa, M., Hashida, M., 1999. Pharmacokinetics of anticancer drugs, plasmid DNA, and their delivery systems in tissue-isolated perfused tumors. Adv. Drug Deliv. Rev. 40, 19–37.

Noguchi, A., Furuno, T., Kawaura, C., Nakanishi, M., 1998. Membrane fusion plays an important role in gene transfection mediated by cationic liposomes. FEBS Lett. 433, 169–173.

Nomura, T., Koreeda, N., Yamashita, F., Takakura, Y., Hashida, M., 1998. Effect of particle size and charge on the disposition of lipid carriers after intratumoral injection into tissue-isolated tumors. Pharm. Res. 15, 128–132.

Pelecanou, M., Pirmettis, I.C., Papadopoulos, M.S., Terzis, A., Chiotellis, E., Stassinopoulou, C.I., 1999. Structural studies of ReO(V) mixed ligand [SNS][Cl] and [SNS][S] complexes. Inorg. Chim. Acta 287, 142–151.

Pirmettis, I.C., Papadopoulos, M.S., Mastrostamatis, S.G., Raptopoulou, C.P., Terzis, A., Chiotellis, E., 1996. Synthesis and characterization of oxotechnetium(V) mixed-ligand complexes containing a tridentate N-substituted bis(2-mercaptoethyl) amine and a monodentate thiol. Inorg. Chem. 35, 1685–1691.

Prestwich, W.V., Nunes, J., Kwok, C.S., 1989. Beta dose point kernels for radionuclides of potential use in radioimmunotherapy. J. Nucl. Med. 30, 1036–1046.

Therien, H.M., Lair, D., Shahum, E., 1990. Liposomal vaccine: influence of antigen association on the kinetics of the humoral response. Vaccine 8, 558–562.

Tomayko, M.M., Reynolds, C.P., 1989. Determination of subcutaneous tumor size in athymic (nude) mice. Cancer Chemother. Pharmacol. 24, 148–154.

Torchilin, V.P., 2005. Recent advances with liposomes as pharmaceutical carriers. Nat. Rev. Drug Discov. 4, 145–160.

Ueno, N.T., Bartholomeusz, C., Xia, W., Anklesaria, P., Bruckheimer, E.M., Mebel, E., Paul, R., Li, S., Yo, G.H., Huang, L., Hung, M.-C., 2002. Systemic gene therapy in human xenograft tumor models by liposomal delivery of the E1A gene. Cancer Res. 62, 6712–6716.

Villaret, D., Glisson, B., Kenady, D., Hanna, E., Carey, M., Gleich, L., Yoo, G.H., Futran, N., Hung, M.-C., Anklesaria, P., Heald, A.E., 2002. A multicenter phase II study of tgDCC-E1A for the intratumoral treatment of patients with recurrent head and neck squamous cell carcinoma. Head Neck 24, 661–669.

Zweit, J., 1996. Radionuclides and carrier molecules for therapy. Phys. Med. Biol. 41, 1905–1914.